Colloidal chemistry-based synthesis of quantized CuInS₂/Se₂ nanoparticles

NADICA D. ABAZOVIĆ[1], DRAGANA J. JOVANOVIĆ[1], MILOVAN M. STOILJKOVIĆ[1#],
MIODRAG N. MITRIĆ[1], SCOTT P. AHRENKIEL[2],
JOVAN M. NEDELJKOVIĆ[1] and MIRJANA I. ČOMOR[1*]

[1]Vinča Institute of Nuclear Sciences, University of Belgrade, P.O. Box 522, 11001 Belgrade, Serbia and [2]South Dakota School of Mines and Technology, Rapid City, South Dakota 57701, USA

Abstract: Ternary chalcogenide nanoparticles, CuInS₂ and CuInSe₂, were synthesized in a high-temperature boiling non-polar organic solvent. X-Ray diffraction analysis revealed that both materials had a tetragonal (chalcopyrite) crystal structure. The morphology of the obtained materials was revealed by transmission electron microscopy. Agglomerated spherical CuInS₂ nanoparticles with broad size distribution in the range from 2 to 20 nm were obtained. In the case of CuInSe₂, isolated particles with a spherical or prismatic shape in the size range from 10 to 25 nm were obtained, as well as agglomerates consisting of much smaller particles with a diameter of about 2–5 nm. The particles with the smallest diameters of both materials exhibited quantum size effects.

Keywords: I–III–VI₂ semiconductors; quantization; X-ray diffraction; optical properties.

INTRODUCTION

I–III–VI₂ compounds such as CuInS₂ and CuInSe₂ (CIS), as well as Cu(In,Ga)(S,Se) (CIGS), are effective light-absorbing materials which can be used in thin-film solar cells, and printable and flexible photovoltaic devices.[1] These materials possess advantageous properties for solar applications since their band gap energy is at the red edge of the visible solar spectrum (bulk CuInS₂ and CuInSe₂ have band gap energies of 1.53 and 1.04 eV, respectively). CuInS₂ and CuInSe₂ are direct band-gap semiconductors with correspondingly high optical absorption coefficients,[2,3] and, contrary to other candidate materials for thin-film

solar cells such as CdTe and amorphous silicon (a-Si:H), they are stable under long-term excitation.[4] The highest theoretical efficiency was predicted for CuInSe$_2$ and CuInS$_2$ (25 and 28.5 %, respectively),[5] but the experimental record (21.5 %) has been achieved with CIGS-based solar cells.[6] This is significantly higher than for either CdTe or a-Si:H based devices.[7]

One of the hurdles currently impeding widespread commercialization of CIS-based solar cells is the difficulty of achieving controlled stoichiometry over large device areas, leading to high manufacturing costs.[8] CIS layers in state-of-the-art devices are deposited by a multistage co-evaporation process in which alternate copper and indium layers are exposed either to a chalcogenide source or hydrogen chalcogenide gas in the reaction chamber.[9,10] This process is time-consuming, the CIS stoichiometry is difficult to control, intermetallic phases can be formed and the content of S or Se can vary significantly in the films.[8,11] Large material losses on the deposition chamber walls also increase the cost. For these reasons, alternative CIS layer deposition strategies are desired.

One approach with the potential to produce CIS layers with controlled stoichiometry without the need for high temperature annealing is to synthesize chemically colloidal CIS nanocrystals dispersed in solvents, creating a paint or ink. Such an approach, of printable CIS inks, makes accessible a range of solution-based processing techniques and may lead to inexpensive fabrication routes for light-absorbing layers.[1] There are reports in the literature concerning the synthesis of I–III–VI$_2$ semiconductor nanocrystals such as CuInS$_2$, CuInSe$_2$ and AgInS$_2$ based on either solvothermal methods or the usage of single organic precursors.[12–17] These approaches generally suffer from relatively low yields, poor crystallinity and poor uniformity in composition and phase of the obtained nanostructures.[3,18] This is not surprising considering that many of these systems have very complicated phase diagrams.[19] However, there are a few recent reports concerning the synthesis of colloidal CuInS$_2$ and CuInSe$_2$ nanocrystals in organic solvents avoiding the usage of single organic precursors.[1,18,20–23]

In this paper, a novel colloidal route for the synthesis of CuInS$_2$ and CuInSe$_2$ nanocrystals in a non-polar solvent is reported. The obtained nanocrystals could be dispersed in various non-polar solvents, becoming thereby suitable for the deposition of uniform, crack-free films onto different substrates. The in detail structural characterization of the synthesized CuInS$_2$ and CuInSe$_2$ nanocrystals was realized using transmission electron microscopy (TEM) and X-ray diffraction (XRD) analysis, while optical characterization was performed using UV–Vis spectroscopy.

EXPERIMENTAL

Materials

Copper(I) acetate (CuAc), indium(III) acetate (In(Ac)$_3$), Se-pellets and trioctylphosphine (TOP) 90 % were purchased from Sigma Aldrich, while 1-octadecene (ODE) and bis(tri-

methylsilyl)sulfide (TMS) were purchased from Fluka. Myristic acid (98 %) was purchased from Alfa-Aeser. Methanol (HPLC grade) and benzene were purchased from Baker. All chemicals were of the highest purity available and were used without further purification. A standard Schlenk line was used for all the syntheses in order to avoid the presence of any oxygen.

Synthesis of CuInS$_2$ and CuInSe$_2$

CuAc (01. mmol), In(Ac)$_3$ (0.1 mmol) and myristic acid (0.4 mmol), together with 6.2 cm^3 of ODE were introduced into a two-neck reaction flask. The flask was immersed in an oil bath at 170 °C and maintained at this temperature for 30 min under an Ar flow. Then, the flask was heated to 300 °C and 10 min after attaining the temperature, either 2 ml of ODE containing TMS (0.30 mmol) or 2 ml of TOP containing Se (0.30 mmol) were injected in order to obtain CuInS$_2$ or CuInSe$_2$, respectively. The reaction mixtures were kept at 300 °C for 30 min and then allowed to cool spontaneously to room temperature. The obtained precipitates were washed three times with methanol and then dispersed in benzene.

Characterization

X-Ray diffraction (XRD) patterns of the samples were recorded using a Bruker D8 Advance diffractometer equipped with a focusing Ge-crystal primary monochromator (Johanson type) that generates CuKα radiation (step time: 6 or 8 s; step: 0.02 or 0.05°). The powder samples were prepared by drying washed precipitates under an Ar flow.

Micro-structural characterization of samples was performed on Hitachi H-7000 FA TEM with a W-filament. Samples were dispersed in benzene, ultrasonicated for one hour and deposited on C-coated Cu grids.

The quantitative chemical analysis of the obtained precipitates was realized by inductively coupled plasma optical emission spectroscopy (ICP–OES) (Spectroflame ICP, 2.5 kW, 27 MHz). Prior to the measurements, the samples were dissolved in hydrochloric acid. The measurements were performed by measuring the intensity of the radiation emitted by each element at specific wavelengths (λ_{em} = 324.754 nm for Cu and 325.609 nm for In). The concentration (in ppm) of both elements were calculated using a series of standard solutions, the results were transformed into the number of atoms of each element. These numbers were used for the determination of the Cu/In ratio in the synthesized samples: 0.55 in CuInS$_2$ and 0.63 in CuInSe$_2$.

Diluted benzene dispersions of synthesized CuInS$_2$ and CuInSe$_2$ were used for optical measurements. For UV/Vis absorption spectrometry, an Evolution 600 UV/Vis spectrophotometer (Thermo Scientific) was used. Emission measurements were performed on a Perkin Elmer LS 45 luminescence spectrometer.

RESULTS AND DISCUSSION

The X-ray diffraction patterns of the synthesized CuInS$_2$ and CuInSe$_2$ are shown in Fig. 1. The XRD pattern shown in Fig. 1a matches well with the literature data for tetragonal (chalcopyrite)[21] CuInS$_2$. The obtained peaks can be assigned to the (112), (200), (204)/(220) and (312)/(116) crystalline planes. The crystalline structure of the synthesized CuInSe$_2$ is presented in Fig. 1b. The main reflections that correspond well with tetragonal (chalcopyrite) CuInSe$_2$ structure can be noticed. First, there is reflection from the (112) plane, then (204)/(220), (312)/(116), (004)/(200) and very weak from the (103) plane. All peaks are slightly

shifted to larger 2θ values compared to literature data,[15] indicating that crystalline lattice parameters are orderly changed, most likely due to the non-stoichiometric ratio between Cu and In and/or the small size of the particles. The sharp peaks at $2\theta < 26°$ can be assigned to TOP/TOPO adsorbed on the surface of the CuInSe$_2$ nanoparticles. In addition, there is a peak denoted with star at about 43° in Figs. 1a and 1b, which can be assigned to either metallic copper[24] or to an indium rich phase (CuIn$_{11}$S$_{17}$).[25]
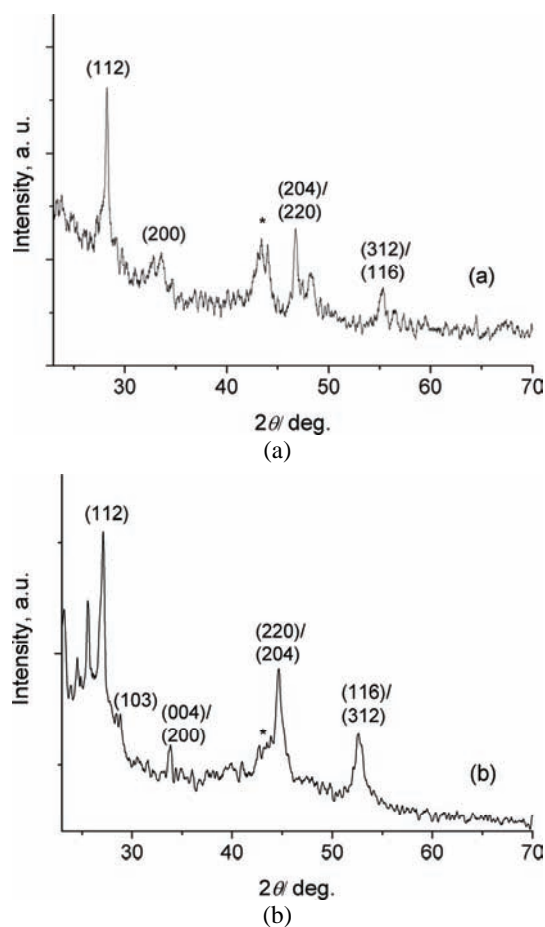

(a)

(b)

Fig. 1. The XRD patterns of a) CuInS$_2$ and b) CuInSe$_2$.

As can be seen from the XRD patterns of both materials, the peaks have an irregular shape – the effect is the most obvious for the (112) peaks, which indicates that crystals of, at least, two sizes were present in the materials. The wide base of the peaks originates from smaller, while the sharp maximum of the peaks corresponds to larger crystallites. The average crystalline domain size of both materials was estimated using XFIT and FOURYA.[26] The grain size was found to be 20 and 15 nm for CuInS$_2$ and CuInSe$_2$, respectively.

The morphology of the CuInS$_2$ and CuInSe$_2$ samples was studied using TEM. Typical TEM images are presented in Fig. 2. Agglomerated spherical CuInS$_2$ nanoparticles with a broad size distribution in the range from 2 to 20 nm can be seen in Fig. 2a. This observation is in agreement with literature data concerning the morphology of CuInS$_2$ synthesized in different ways.[13,15] Practically, it was impossible to find isolated particles due to the usage of a non-coordinating solvent (ODE), which cannot act as a surfactant and prevent aggregation of the particles. The best observation is presented in the inset of Fig. 2a; a small fraction of nearly mono dispersed particles of about 8 nm in diameter is presented. Unfortunately, TEM images of CuInS$_2$ could not be used for size distribution statistics because of the agglomeration. The CuInSe$_2$ nanoparticles were much better dispersed on the grid (Fig. 2b). The size distribution was broad (2–25 nm), and isolated particles with spherical or prismatic shape can be seen. The size distribution statistics was performed and the results are presented in Figs. 2c and 2d. The larger fraction of spherical and prismatic particles has sizes of about 13 nm, smaller particles organized as agglomerates have diameters ≤ 5 nm. The observed morphologies are the consequence of the growth mechanism. As pointed out in the literature,[21] after formation of the primary particles, the growth proceeds through Ostwald ripening and aggregation. For Ostwald ripening, a complexion agent is necessary (in the present case, it is myristic acid) and if it is not present the growth can proceed only through aggregation. It should be mentioned that there is reasonably good agreement in the size estimation from TEM and XRD measurements.
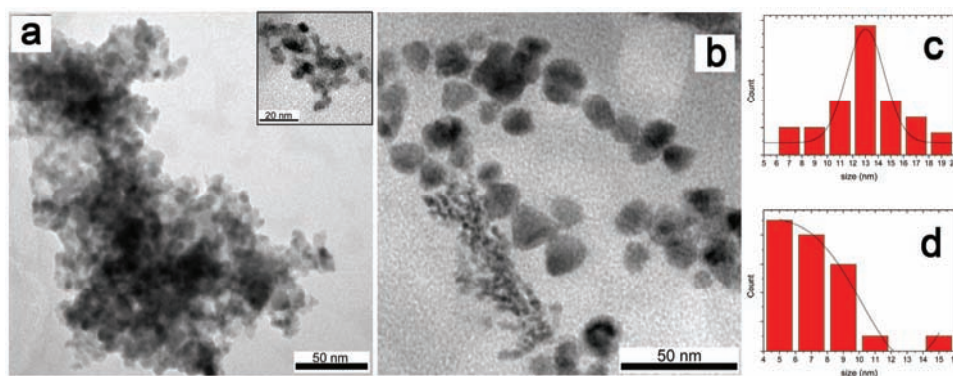

Fig. 2. Typical TEM images of a) CuInS$_2$ and b) CuInSe$_2$, and the size distribution histograms (c and d) of the CuInSe$_2$ nanoparticles.

The absorption onset of each product was determined by a least-squares fit of the linear region of a $(Ah\nu)^2$ *vs.* $h\nu$ plot (A = absorbance, h = Planck's constant, and ν = frequency), as presented in Fig. 3. Due to the position of their absorption threshold, band gaps of 2.02 eV for CuInS$_2$ and 2.13 eV for CuInSe$_2$
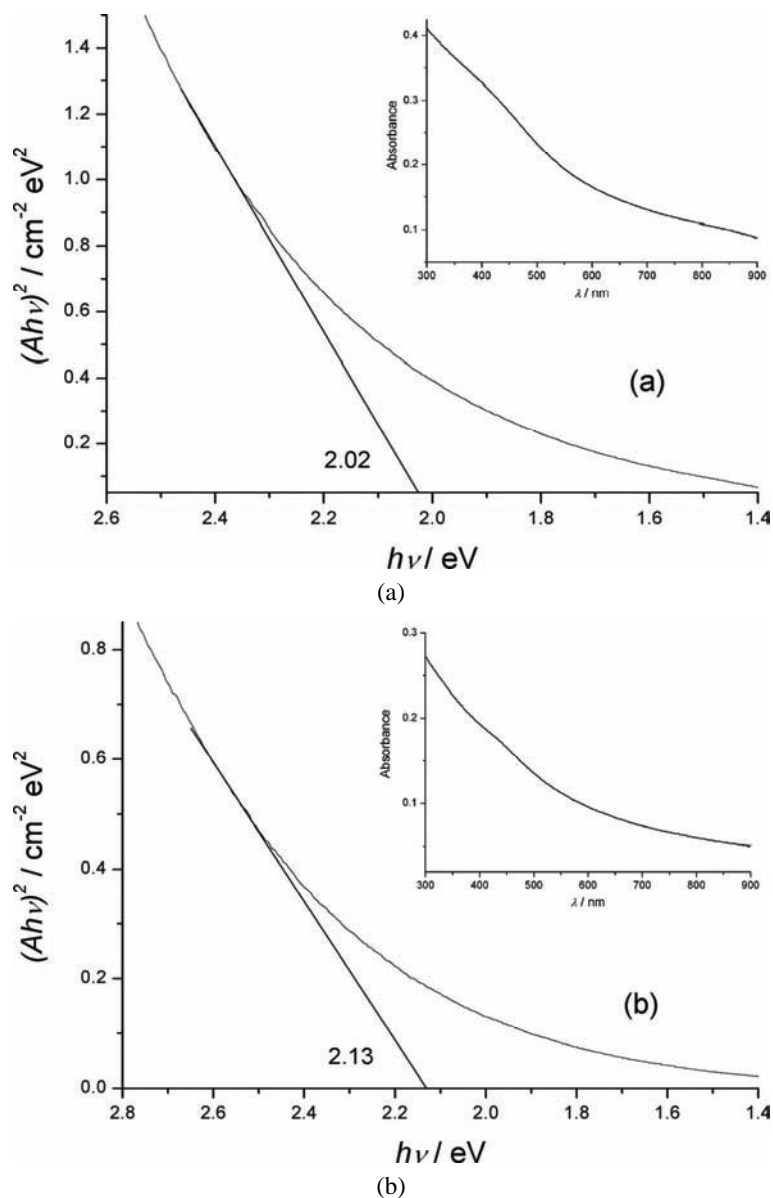
(a)

(b)

Fig. 3. Plots of $(Ah\nu)^2$ *vs.* energy for a) CuInS$_2$ and b) CuInSe$_2$ nanoparticles. The insets show the absorption spectrum of the corresponding colloidal dispersions.

are obtained. In order to correlate the optical properties of the synthesized nanoparticles of both materials with size, the effective mass approximation model (Eq. (1)) was used to calculate the size of the particles from the increase of the effective band gap energies:[27]

$$\Delta E = \frac{\hbar^2 \pi^2}{2R^2}\left(\frac{1}{m_e} + \frac{1}{m_h}\right) - \frac{1.8e^2}{\varepsilon R} \tag{1}$$

where ΔE is the increase of the band gap energy, m_e and m_h are the effective masses of electrons and holes, respectively, ε is the dielectric constant and R is the radius. Values for CuInS₂ ($m_e = 0.16$, $m_h = 1.3$ and $\varepsilon = 11$) and CuInSe₂ ($m_e = 0.082$, $m_h = 0.71$ and $\varepsilon = 15$) were taken from literature.[15] The increase of the band gap energy (ΔE) was estimated to be 0.5 and 1 eV for CuInS₂ and CuInSe₂, respectively. Using these values, the calculated diameters of the nanoparticles were found to be about 2 and 3 nm for CuInS₂ and CuInSe₂, respectively. Although these values are smaller compared to values estimated from the TEM measurements, it should be emphasized that they are similar to the size of the primary particles of which the larger agglomerates are composed. The absorption spectra were obtained using benzene dispersions of the obtained samples where agglomeration is negligible.

Theoretical calculations have shown that the Wannier–Mott bulk exciton radiuses are 4.1 and 10.6 nm for CuInS₂ and CuInSe₂, respectively.[15] According to particle sizing performed by TEM and XRD, the smallest particles of both materials should be in the weak confinement regime and quantum effects due to reduced dimensionality could be expected. The optical characterization also revealed quantum confinement. The absorption spectra of dispersed CuInS₂ and CuInSe₂ are shown in the insets in Figure 3. In both cases, rather featureless absorption spectra were obtained with tail towards the infrared region and a shoulder in the spectral range 400 to 500 nm. The presence of the absorption tail can be explained by light scattering due to the presence of agglomerated particles. On the other hand, the presence of shoulder instead of a well-resolved exciton band is the consequence of the rather broad size distributions of the CuInS₂ and CuInSe₂ nanoparticles.

In order to reveal the ratio between copper and indium in the synthesized materials, assuming that peaks marked with a star in Figs. 1a and 1b can be assigned to non-stoichiometric In rich compounds, ICP–OES measurements were performed. One of the most attractive properties of CuIn(S,Se) compounds is that they appear to tolerate a large range of anion-to-cation off stoichiometry, which is manifested by the existence of a series of ordered defect compounds (ODC) with large variations in their Cu/In/(S,Se) atomic ratios.[28] These ODCs generally possess wider band gap and type of conductivity can be changed with changes of Cu/In ratio from p to n. The measurements indicated Cu/In ratios of about 0.55 and 0.63 for CuInS₂ and CuInSe₂, respectively. Both materials are indium-rich and consequently n-type conductivity can be expected.[29]

The materials obtained in this study showed no detectable emission, contrary to literature data.[21] The nature of the surface ligands plays an important role in

the PL efficiency of CuIn(S,Se)$_2$ nanocrystals, as was shown by Castro *et al.*[13] Obviously the choice of non-coordinating solvent/surfactants (ODE/TOP) proved themselves excellent for quenching emission and making the photogenerated charges more available for use in photovoltaic devices. This will be the subject of future experiments.

CONCLUSIONS

A simple synthetic procedure for the preparation of CuInS$_2$ and CuInSe$_2$ nanoparticles has been presented. The obtained materials had a tetragonal (chalcopyrite) crystalline structure. XRD results indicated broad particle size distributions, all in nano dimensions. TEM measurements also revealed the presence of nanoparticles of different dimensions and a tendency of the CuInS$_2$ nanoparticles to form agglomerates. The particles of smallest dimensions of both materials exhibit size quantization effects due to reduced dimensionality. The effective mass approximation model was used to correlate the optical properties of the obtained colloidal nanoparticles with their diameters.

И З В О Д

СИНТЕЗА КВАНТИЗИРАНИХ НАНОЧЕСТИЦА CuInS$_2$/Se$_2$ КОЛОИДНО-ХЕМИЈСКОМ МЕТОДОМ

НАДИЦА Д. АБАЗОВИЋ[1], ДРАГАНА Ј. ЈОВАНОВИЋ[1], МИЛОВАН М. СТОИЉКОВИЋ[1], МИОДРАГ Н. МИТРИЋ[1], SCOTT P. AHRENKIEL[2], ЈОВАН М. НЕДЕЉКОВИЋ[1] и МИРЈАНА И. ЧОМОР[1]

[1]Институт за нуклеарне науке "Винча", Универзитет у Београду, п. пр. 522, 11001 Београд и [2]South Dakota School of Mines and Technology, Rapid City, South Dakota 57701, USA

Наночестице тернарних халкогенида, CuInS$_2$ и CuInSe$_2$, синтетисане су у неполарним, органским растварачима високе тачке кључања. Дифракција X-зрака показала је да оба материјала имају тетрагоналну (халкопиритну) кристалну структуру. Употребом трансмисионе електронске микроскопије откривено је да су честице сферног облика нано-димензија. Наночестице CuInS$_2$ формирају агрегате и имају широку расподелу величина честица од 2–20 nm. У случају CuInSe$_2$, добијене су изоловане честице сферног и призматичног облика, димензија од 10–25 nm као и агломерати који се састоје од честица знатно мањих димензија, од 2–5 nm. Оба материјала показују квантизациони ефекат услед нанодимензија.

(Примљено 10. априла, ревидирано 13. децембра 2011)

REFERENCES

1. M. G. Panthani, V. Akhavan, B. Goodfellow, J. P. Schmidtke, L. Dunn, A. Dobadalapur, P. F. Barbara, B. A. Korgel, *J. Am. Chem. Soc.* **130** (2008) 16770
2. W. E. Devaney, W. S. Chen, J. M. Stewart, R. A. Mickelsen, *IEEE Trans. Electron Devices* **37** (1990) 428
3. R. Scheer, T. Walter, H. W. Schock, M. L. Fearheiley, H. J. Lewerenz, *Appl. Phys. Lett.* **63** (1993) 3294

4. J.-F. Guillemoles, L. Kronik, D. Cahen, U. Rau, A. Jasenek, H.-W. Schock, *J. Phys. Chem., B* **104** (2000) 4849
5. S. Siebentritt, *Thin Solid Films* **403**–**404** (2002) 1
6. J. S. Ward, K. Ramanathan, F. S. Hasoon, T. J. Coutts, J. Keane, M. A. Contreras, T. Moriarty, R. Noufi, *Prog. Photovoltaics Res. Appl.* **10** (2002) 41
7. M. A. Green, K. Emery, D. L. King, Y. Hishikawa, W. Warta, *Prog. Photovoltaics Res. Appl.* **15** (2007) 35
8. M. Powalla, B. Dimmler, *Thin Solid Films* **361**–**362** (2000) 540
9. I. Repins, M. A. Contreras, B. Egaas, C. De Hart, J. Scharf, C. L. Perkins, B. To, R. Noufi, *Prog. Photovoltaics Res. Appl.* **16** (2008) 235
10. A. Contreras, B. Egaas, K. Ramanathan, J. Hiltner, A. Swartzlander, F. Hasoon, R. Noufi, *Prog. Photovoltaics Res. Appl.* **7** (1999) 311
11. H.-W. Schock, R. Noufi, *Prog. Prog. Photovoltaics Res. Appl.* **8** (2000) 151
12. H. I. Elim, W. Ji, M.-T. Ng, J. J. Vittal, *Appl. Phys. Lett.* **90** (2007) 033106
13. S. L. Castro, S. G. Bailey, R. P. Raffaelle, K. K. Banger, A. F. Hepp, *J. Phys. Chem., B* **108** (2004) 12429
14. K. K. Banger, M. H.-C. Jin, J. D. Harris, P. E. Fanwick, A. F. Hepp, *Inorg. Chem.* **42** (2003) 7713
15. S. L. Castro, S. G. Bailey, R. P. Raffaelle, K. K. Banger, A. F. Hepp, *Chem. Mater.* **15** (2003) 3142
16. B. Li, Y. Xie, J. Huang, Y. Qian, *Adv. Mater.* **11** (1999) 1456
17. C. Czekelius, M. Hilgendorff, L. Spanhel, I. Bedja, M. Lerch, G. Müller, U. Bloeck, D.-S. Su, M. Giersig, *Adv. Mater.* **11** (1999) 643
18. S.-H. Choi, E.-G. Kim, T. Hyeon, *J. Am. Chem. Soc.* **128** (2006) 2520
19. A. Ghezelbash, B. A. Korgel, *Langmuir* **21** (2005) 9451
20. M. A. Malik, P. O'Brien, N. Revaprasadu, *Adv. Mater.* **11** (1999) 1441
21. H. Zhong, Y. Zhou, M. Ye, Y. He, J. Ye, C. He, C. Yang, Y. Li, *Chem. Mater.* **20** (2008) 6434
22. M. Kruszynska, H. Borchert, J. Parisi, J. Kolny-Olesiak, *J. Am. Chem. Soc.* **132** (2010) 15976
23. K. Nose, T. Omata, S. Otsuka-Yao-Matsuo, *J. Phys. Chem., C* **113** (2009) 3455
24. M. Salavati-Niasari, F. Davar, *Mat. Lett.* **63** (2009) 441
25. R. P. Wijesundera, W. Siripala, *Sol. Energy Mater. Sol. Cells* **81** (2004) 147
26. R. W. Cheary, A. A. Coelho, *Programs XFIT and FOURYA*, deposited in CCP14 Powder Diffraction Library, Engineering and Physical Sciences Research Council, Daresbury Laboratory, Warrington, England, http://www.ccp14.ac.uk/tutorial/xfit-95/xfit.htm (1996)
27. L. Brus, *J. Phys. Chem.* **90** (1986) 2555
28. R. R. Philip, B. Pradeep, *Thin Solid Films* **472** (2005) 136
29. K. Yoshino, K. Nomoto, A. Kinoshita, T. Ikari, Y. Akaki, T. Yoshitake, *J. Mater. Sci. Mater. Electron.* **19** (2008) 301.